

Numerical Analysis of Wavelength Conversion Based on Semiconductor Optical Amplifier Integrated with Microring Resonator Notch Filter

Mohammad Razaghi^a, Mojtaba Gandomkar^b, Vahid Ahmadi^b, Narottam Das^c and Michael J. Connelly^d

^a Dept. of Electrical and Computer Eng., University of Kurdistan, Sanandaj, Iran, Email: m.razaghi@uok.ac.ir

^b Dept. of Electrical and Computer Eng., Tarbiat Modares University, Tehran, Iran

^c Electron Science Research Institute, Edith Cowan University, Joondalup, WA 6027, Australia

^d Dept. of Electronic & Computer Eng., University of Limerick, Limerick, Ireland

Abstract— In this paper, we numerically investigate the wavelength conversion using semiconductor optical amplifier (SOA) integrated with microring resonator. In the model all nonlinear effects, which can appear in picosecond and subpicosecond pulse regime, are taken into account. It is shown that with three coupled microring resonators, output four-wave mixing (FWM) signal generated by the SOA can be filtered perfectly. Moreover, it is demonstrated that microring resonator can be used for modifying the output FWM signal shape and spectrum. The output time bandwidth product is also enhanced by this technique.

I. INTRODUCTION

All optical wavelength converters are the important key elements in ultrafast optical communication systems [1]. Among different schemes for high-speed wavelength conversion, using wave-mixing technique for generating four-wave mixing (FWM) signals in semiconductor optical amplifiers (SOAs) is a promising choice due to its inherent ultrafast nonlinearities [2].

As the input pulsewidth become comparable to picoseconds, besides self-phase modulation (SPM), which has the dominant effects on propagated signal, other nonlinear phenomenon, such as, ultrafast nonlinear refraction index (UNRI), spectral hole burning (SHB), carrier heating (CH), two photon absorption (TPA) and Kerr effects change the characteristics of SOA's output signal shape and spectrum. There are different methods reported to reshape the output signal [3-4].

The schematic diagram of the proposed system is shown in Fig. 1. The wavelength converter consists of an SOA and an integrated passive microring resonator including three microrings. This structure can filter the output FWM signal of the SOA and suppress high power pump and probe energy at the output. It has also been shown that the microring resonator can reduce the side effects of SOA's nonlinearities and its output signal becomes more symmetric in comparison with the SOA's output FWM signal.

II. NUMERICAL MODEL

To include all the mentioned nonlinear effects in the SOA, modified nonlinear Schrödinger equation (MNLSE) is used [2]:

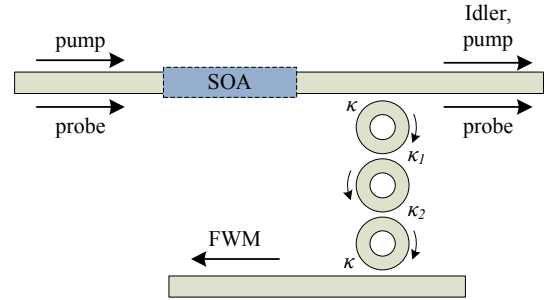


Fig. 1. Schematic diagram of the proposed wavelength converter system.

$$\left[\frac{\partial}{\partial z} - \frac{i}{2} \beta_2 \frac{\partial^2}{\partial \tau^2} + \frac{\gamma}{2} + \left(\frac{\gamma_{2p}}{2} + ib_2 \right) |V(z, \tau)|^2 \right] V(z, \tau) = \left\{ \frac{1}{2} g_N(\tau) \left[\frac{1}{f(\tau)} + i\alpha_N \right] + \frac{1}{2} \Delta g_T(\tau) (1 + i\alpha_T) - i \frac{1}{2} \frac{\partial g(\tau, \omega)}{\partial \omega} \Big|_{\omega_0} \frac{\partial}{\partial \tau} - \frac{1}{4} \frac{\partial^2 g(\tau, \omega)}{\partial \omega^2} \Big|_{\omega_0} \frac{\partial^2}{\partial \tau^2} \right\} V(z, \tau) \quad (1)$$

where, τ is the frame of local time. $V(z, \tau)$ is the slowly varying envelope function of the optical signal pulse, β_2 is the group velocity dispersion (GVD), γ is linear loss, γ_{2p} is the TPA coefficient, b_2 is the instantaneous SPM term due to the Kerr effect. $g_N(\tau)$ is the saturated gain due to carrier depletion (CD), g_0 is the linear gain, $f(\tau)$ is the SHB function, α_N and α_T are the linewidth enhancement factors associated with the gain changes due to the CD and CH, respectively. $\Delta g_T(\tau)$ is the resulting gain change due to the CH and TPA.

For solving Eq. 1, the SOA cavity is divided to M equal sections. By using a central-difference approximation in time domain and trapezoidal integration over spatial section and applying an iterative procedure, a set of MNLSEs can be solved with high precision in few seconds [2].

Wave propagation equation in microrings is simulated utilizing finite-difference time domain (FDTD) method. This equation in the simplest form is

$$\left(\frac{1}{v_g} \frac{\partial}{\partial t} + \frac{\partial}{\partial z} \right) V(z, t) = 0 \quad (2)$$

where, v_g is the group velocity and we assume $v_g = 80$ ($\mu\text{m}/\text{ps}$). After traveling half of the periphery of the ring (length between coupling points), an additional phase $2\pi^2 n_{\text{eff}} \lambda_0$ is added to $V(z, t)$ where λ_0 is the central wavelength of optical signal pulse.

III. RESULTS

The applicability and precision of the SOA model have been validated through comparison with experimental results [3]. The material parameters used in the simulation are taken from [3]. The input signal shape is sech^2 and is Fourier transform limited. The duration of input signal pulses are varied from 5 ps to 20 ps. The input probe energies are varied 0.2 pJ to 1.6 pJ. The pump pulse energy is 10 times stronger than the probe pulse energy. The detuning frequency between the input pump and probe is 1 THz.

To filter out all the signals except the FWM signal, three microrings are cascaded (as shown in Fig. 1). This provides the required out-of-band signal rejection to eliminate the pump energy from the output. The coupling coefficients between waveguides are selected to realize a maximally flat bandpass filter. This means that it satisfies the condition $\kappa_1^2 = \kappa_2^2 = 0.125\kappa^4$ [5] where, κ_1 and κ_2 are the coupling coefficients between two microrings and κ is coupling coefficient between each straight waveguide and its nearby microring. Here, $\kappa = 0.3$ and radii of microrings are equal to $R = 2.5$ (μm). The effective refractive index of the ring waveguide is $n_{\text{eff}} = 3$.

The output FWM signal spectra of both the SOA and microring are shown in Fig. 2, for probe signal pulse energy of 1.6 pJ and pulsewidth of 5 ps. As it is depicted, the microring's output FWM signal spectral width is decreased because of the narrow filter imposed by the microring structure. Besides, the oscillatory phenomena, which are due to SOA nonlinearities are removed from the FWM spectrum by this technique. As a result, the output FWM signal shape and spectrum of the microring are more symmetric in comparison with SOA's output FWM signal. Fig. 3 shows the output FWM signal shape of the SOA and microring corresponding to the Fig. 2. Based on the results, microring filters perfectly the FWM signal. Furthermore, it suppresses the SOA nonlinearities and makes the FWM signal more symmetric. Besides, the time bandwidth product (TBP) of the SOA's output FWM signal decreases from 0.5 to 0.45 in microring's output FWM signal.

Fig. 4 shows the output spectral width of both FWM signal of SOA and microring for different input pulsewidths and energies. As the microring bandwidth is 50 GHz, the FWM signal spectrum is compressed to more than half of SOA's

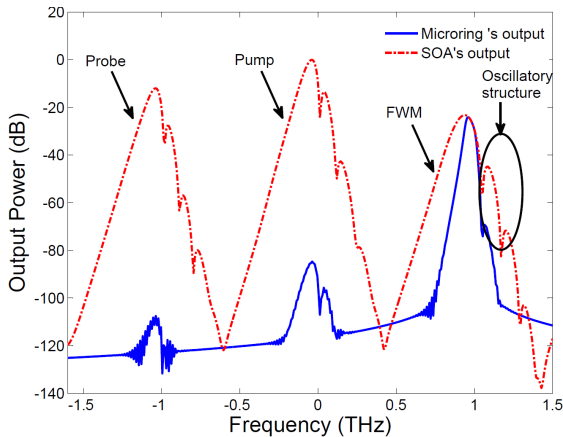


Fig. 2. Output spectra of the SOA and the microring.

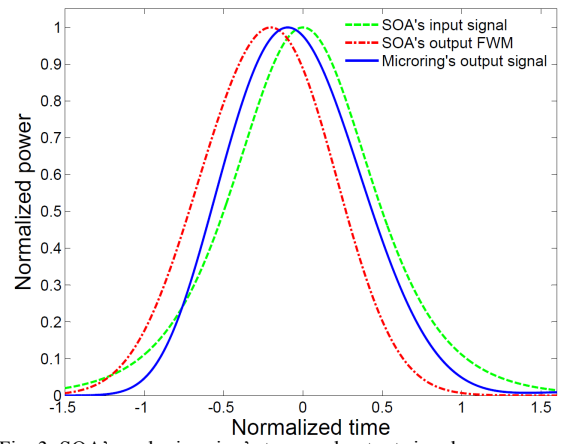


Fig. 3. SOA's and microring's temporal output signal power versus normalized time. The time scale is normalized to pulsewidth of each corresponding signal.

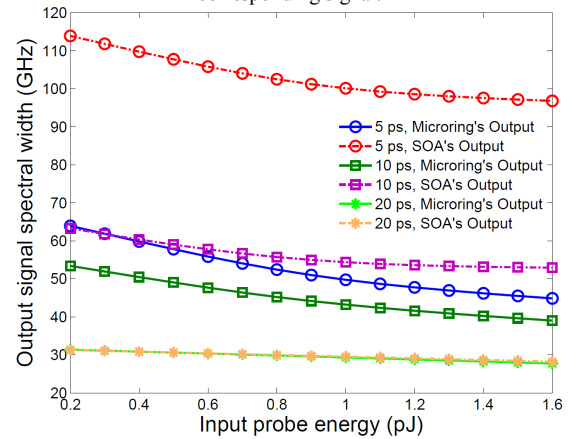


Fig. 4. SOA's and microring's output signal spectral width for different input pulsewidths versus input probe energy characteristics.

output FWM signal for some cases. For larger input pulsewidths, as the spectral width decreases inherently the effects microring reduced consequently.

IV. CONCLUSION

Numerical modeling of wavelength conversion using SOA and integrated microring notch filter was studied in this paper. It has shown microring resonator in addition to FWM signal filtering, enhances some of its characteristics, such as temporal signal shape symmetry, TBP. Moreover, microring leads to the compression of FWM signal spectral width.

References

- [1] C. Meuer et. al, "80 Gb/s wavelength conversion using a quantum-dot semiconductor optical amplifier and optical filtering," *Opt. Express*, vol. 19, pp. 5134-5142, 2011.
- [2] N. K. Das, Y. Yamayoshi, and H. Kawaguchi, "Analysis of basic four-wave mixing characteristics in a semiconductor optical amplifier by the finite-difference beam propagation method," *IEEE J. Quantum Electron.*, vol. 36, no. 10, pp. 1184-1192, Oct. 2000.
- [3] M. Razaghi, V. Ahmadi and M. J. Connelly, "Comprehensive finite-difference time-dependent beam propagation model of counterpropagating picosecond pulses in a semiconductor optical amplifier," *IEEE Journal of Lightwave Technology*, vol. 27, No. 15, pp. 3162-3174, 2009.
- [4] M. Razaghi, V. Ahmadi and M. J. Connelly, "Femtosecond pulse shaping using counter-propagating pulses in a semiconductor optical amplifier". *Opt. Quant. Electron.*, Springer, 2009.
- [5] B. E. Little, S. T. Chu, H. A. Haus, J. Foresi, and J. P. Laine, "Microring resonator channel dropping filters," *Journal of Lightwave Technology*, vol. 15, pp. 998-1005, 1997.